2017

Numerical Assessment Approach for Flange to Flange Double Tee Connections Subject to Vehicular Loading

Robin Hendricks
Lehigh University

NUMERICAL ASSESSMENT APPROACH FOR FLANGE TO FLANGE DOUBLE TEE CONNECTIONS SUBJECT TO VEHICULAR LOADING

By
Robin J. Hendricks

A Thesis
Presented to the Graduate and Research Committee
of Lehigh University
in Candidacy for the Degree of

Master of Science
in
Structural Engineering

Lehigh University
May, 2017

This thesis is accepted and approved in partial fulfillment of the requirements for the Master of Science

---

Date: May 5, 2017

Thesis Advisor: Dr. Clay J. Naito

Chairperson of Department: Dr. Panos Diplas

ACKNOWLEDGEMENT

I would like to thank my thesis advisor Dr. Clay Naito for the excellent guidance and help with all aspects of the research and testing that went into this project. I would also like to thank my wife Abigail Synnestvedt for all the encouragement, advice, and moral support that she provided. I would like to thank my parents, Steve and Denise, for always encouraging me to advance my knowledge. I started this graduate program under the encouragement of the late Frank Stokes and I'm thankful that he encouraged me to start the process.

This research project was a highly collaborative effort, and so I'd like to thank Andrew Osborn of WJE and Dr. Greg Lucier of North Carolina State University for their many contributions, including making test data and pictures from their test programs available for analysis.

I would also like to recognize that the experimental studies conducted as part of the research effort were funded by the Precast/Prestressed Concrete Institute. Connector hardware material was donated by manufacturers. Many individuals on the PCI technical advisory committee contributed to the research effort including: Roger Becker, Ned Cleland, Larbi Senour, Harry Gleich, Chuck Wynings, Chuck Magnesio, and Steven Altstadt.

CONTENTS

LIST OF TABLES

LIST OF FIGURES

ABSTRACT

A PCI funded research effort was conducted to assess the fatigue resistance of welded flange to flange connections used in double tee precast concrete construction. The connection consists of steel connectors embedded in the edge of the precast flange welded to each other through the use of a steel jumper plate and fillet welds. Variations on this connection have been used for over 50 years with success. The strength limit states of this connection have been explored in detail but the stresses in the connection at service load levels are not well understood. The research effort was conducted specifically to quantify the fatigue resistance of these connections to the repeated loading typical of parking structure service demands. A two part series of articles are developed to summarize methods that can be used to accurately analyze and assess the fatigue life of these connections. This paper examines numerical methods that can be used to readily determine the state of stress in the weld under service loads using detailed 3D models of connector systems and shell element models of diaphragm systems. The ability to accurately determine the stresses in the weld can be combined with a vehicular load spectrum and a suitable fatigue life curve for the fillet weld detail to obtain a realistic assessment of the fatigue life of connections.

BACKGROUND AND INTRODUCTION

For over 50 years, prestressed concrete double tee members have been the component of choice for parking structures throughout the United States. The double tee members are laid side by side and typically span approximately 60 ft. The 60 ft span is desirable because it provides a column free span over two drive aisle lanes flanked on both sides by parking stalls[1]. Double tee (DT) floor systems can be topped in the field with cast-in-place concrete or manufactured with the appropriate strength and surface conditions to eliminate the need for field placed topping. These two types of systems are referred to as topped and untopped (or pre-topped) double tee diaphragms. Untopped systems are predominantly attached using welded mechanical connections. These connections provide integrity for the floor by providing shear and axial force transfer and allow for a means of achieving vertical alignment between adjacent tees. Some systems are developed with welded connections intended for shear only, or for tension in chord connections. These systems may include cast-in-place concrete strips (wet connections) or robust mechanical dry connections at the double tee ends for chords where higher strength or deformation demand are critical (Figure 1).

To provide lateral continuity between pretopped double tees, away from ends, weld plate connections have typically been used. For pretopped double tees, earlier connections were plant-fabricated plates with headed studs, deformed bar anchors, or welded rebar for anchorage into the flange. The double tees were joined using a round bar or rectangular plate, also called a jumper plate, erection plate or slug, welded to the embedded flat plates (Figure 2a and b). Starting around 1976, proprietary connection hardware began to be

marketed and sold in the US (Figure 2c and d). The original proprietary connections were made from galvanized mild steel. Increasingly, in northern climates subject to road salts, the connections have been fabricated from stainless steel. Three common manufactured connectors used in the US today are illustrated in Figure 3.

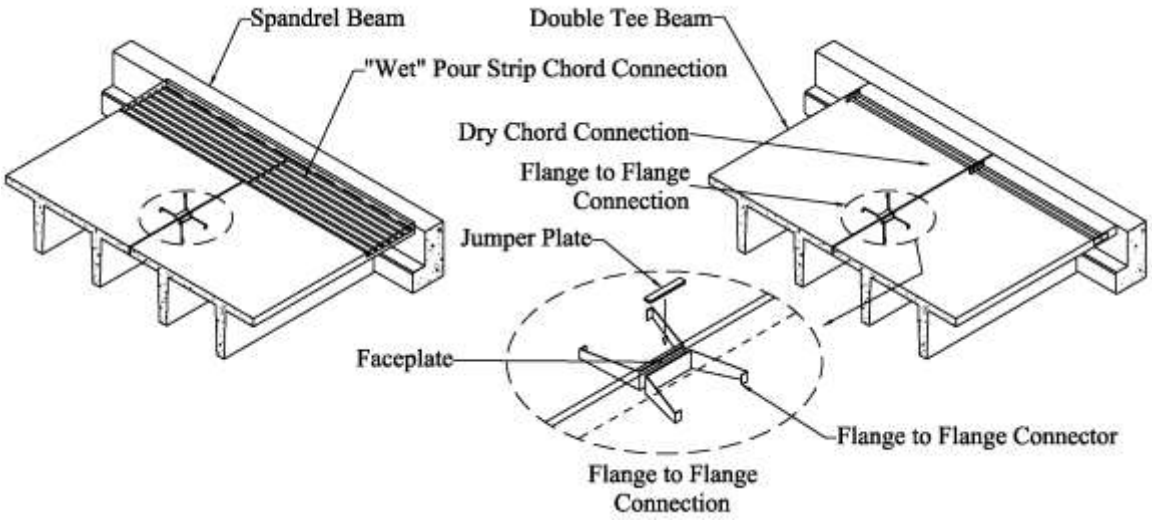

Figure 1: Precast double tee connections

Manufactured flange connections all have similarities in that they all consist of a faceplate with integral legs that are embedded in the concrete and are connected by a jumper plate with a fillet weld on each side. The fillet weld is applied on the top surface of the jumper plate only and this configuration can result in bending stresses on the weld throat with the root of the weld in tension. The most common type of jumper plate is 0.375 in. thick, 2.5 to 3.5 in. long, and 0.5 to 2 in. wide. Round slugs of similar dimensions are sometimes used instead of plates (Figure 2b). Jumper plate widths and slug diameters are adjusted to accommodate variable joint gaps between double tees, but are typically about 1 in. wide. Connections are usually spaced 5ft. to 8 ft. on center along the joint with closer spacing

sometimes used at the midspan of the double tees.

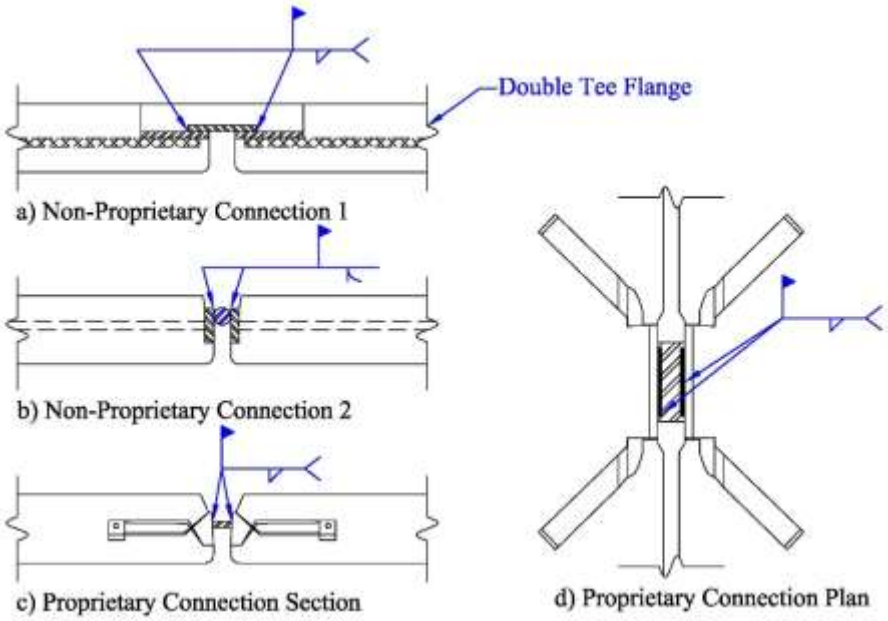

Figure 2: Proprietary and non-proprietary flange connections

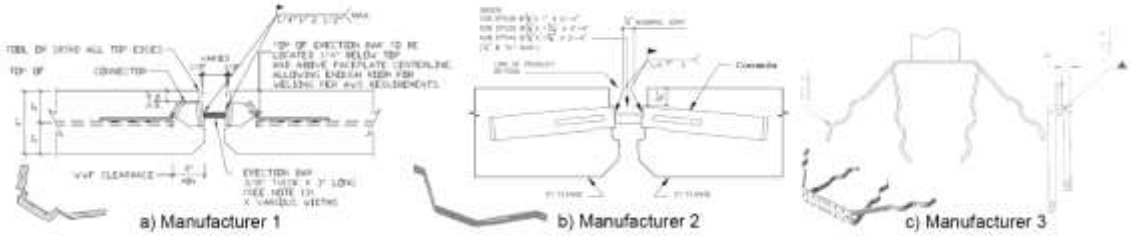

Figure 3: Proprietary connectors currently available in the marketplace

Significant amount of research has been conducted to assess the performance of DT flange connections under strength levels. Early testing was performed by Venuti[2], Spencer and Neille[3], and Aswad[4] on non-proprietary connections and continued on manufactured connections by Pincheira et al.[5], Oliva[6], WJE[7], Shaikh and Fiele[8], Naito[9], and Naito and Hendricks[10]. Testing consisted of in-plane shear and tension and out-of-plane shear forces across the joint. A large number of the studies are summarized in Ren and Naito[11]. The focus of the majority of these studies was to determine the capacity of the connections for design purposes. Research was also conducted to assess the stiffness and ductility to in-

plane shear and axial loads to assess the response of these connections under seismic demands[12,13]. Due to the complexity of the load path through manufactured connections experimental testing is conventionally used over closed form calculations to determine connector strength limit states[14]. Consequently, detailed mechanics of the individual connectors is not well understood. At service level loading, research has been limited to studies by Klein and Lindenberg[15] which explored the deformation levels generated in DT floor diaphragms due to thermal variations. While significant efforts have been conducted to ensure the performance of connections under strength and thermal limit states, assessment of fatigue limit states have not been examined.

Cyclic connector loading arises from differential flange deflections caused by vehicles crossing the flange joints as shown in Figure 4. To properly assess the fatigue resistance of the connection requires a knowledge of: (1) the relationship between the applied vehicle load and the resulting stresses in the connection welds, (2) the expected vehicle demands and distributions in the structure over the expected service life, and (3) an S-N curve that is applicable for the weld being considered. With a proper understanding of these three pieces, any combination of connections and vehicle loads can be examined to assess the likelihood of fatigue induced fracture of connection welds. This paper focuses on the development and validation of a methodology for determination of weld stresses in connections due to applied vehicle loads.

Connection Evaluation Methodology

Simple approaches have been used in the past to approximate the strength of connections for design. The first edition of the PCI Connections Manual[16] for example assumes that

vehicle loads impart only shear on the connection weld (eccentricity between welds are ignored). Other approaches attempt to incorporate both the shear and resulting flexure that is introduced across the jumper plates. This can range from the assumption that the jumper plate is rigid and all deformation takes place in the faceplate (Figure 4d) to a case where the faceplate of the connection is assumed rigid and all deformation takes place in the jumper plate (Figure 4e). Due to the relative flexibility of the faceplate, weld and jumper plate the actual response is much more complicated. As illustrated in the finite element analysis shown in Figure 4f, the stresses that arise in conventional connector systems due to vehicle loading vary in three dimensions and are beyond the scope of traditional hand analysis.

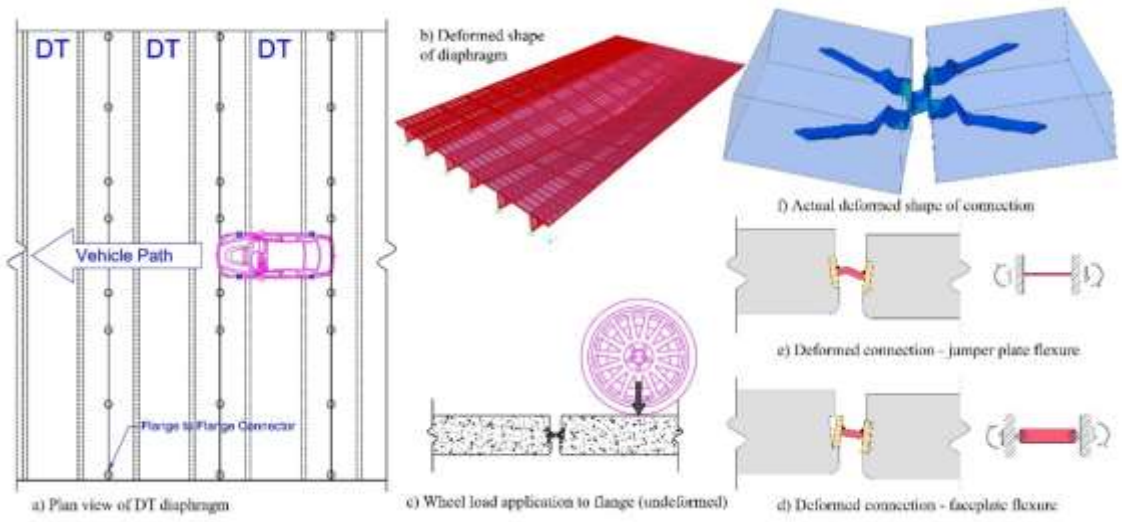

Figure 4: Differential flange deflections due to vehicular loading

Three dimensional finite element analysis of the entire diaphragm system provides the most accurate modeling approach for assessment of connector response. These models can be very complex and computationally expensive. In addition modeling all discrete connections of an entire diaprhagm does not lend itself to assessment of the wide variations

in diaphragm configuraions that are present in current construction. A simplified numerical method is proposed that can be used to accurately determine the stresses in flange to flange connections (Figure 5). As a first step the stiffness of the connection is determined from a detailed three dimensional (3D) finite element model of the local system. In the second step the connector stiffness is used in a shell model of a diaphgragm system with the connectors replaced by linear uncoupled springs to determine the connection deformation under loading. The final step consists of application of the differential displacements and rotations to the initial 3D FE model to determine the actual stresses in the weld under loading. These stresses can then be used with an appropriate S-N curve to determine the likelihood of fatigue induced fracture. The modeling approach proposed is validated by experimental data acquired from full scale connector component tests and welded connection double tee tests.

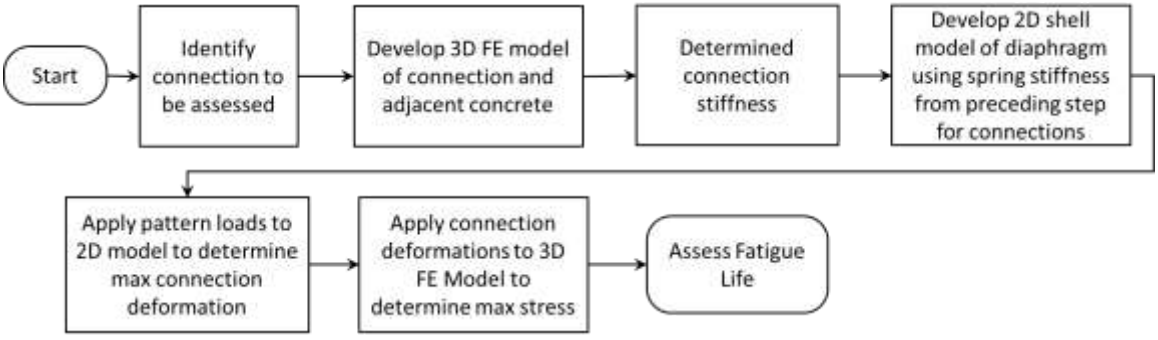

Figure 5: Connection assessment methodology

DEVELOPMENT AND VALIDATION OF 3D FINITE ELEMENT MODEL

Development of an accurate 3D FE model is critical to the approach proposed. Many commercial codes are available for development of such a model, however due to the complexity of the model, validation is necessary. The 3D models utilized were developed

using ABAQUS version 6.13[17]. To examine the accuracy of the 3D modeling approach a series of component tests were conducted to measure the response of full scale connections.

Component Tests on Full Scale Connections

Single sided connector tests were performed with the goal of calibrating detailed 3D finite element models of the connectors. The connectors were loaded at an eccentricity of 1.0 in. from the face of the connector and applied load, vertical displacement, loading block rotation, and strains in at least three locations were recorded throughout the test. The connectors were loaded in force increments of 300 lbs. up to 1500 lbs. and then monotonically loaded to failure. Three cycles were applied at each force level with application at a quasi-static rate.

The tests evaluated the response of connectors subjected to vertical shear. Half of the connection was evaluated, in that one embedded connector was tested with a slug and a loading fixture. The test setup is shown in Figure 6. A slug was attached to a single embedded connector. The slug was oversized to allow attachment to a loading head. The test fixture was manufactured such that the center of vertical shear was at 1.0 in. from the face of the connector. A series of strain gages were included on the face of the connector, vertical displacement was measured using a transducer attached to the loading head. Rotation of the loading head was also monitored using a tilt gage mounted to the loading head as illustrated in Figure 6.

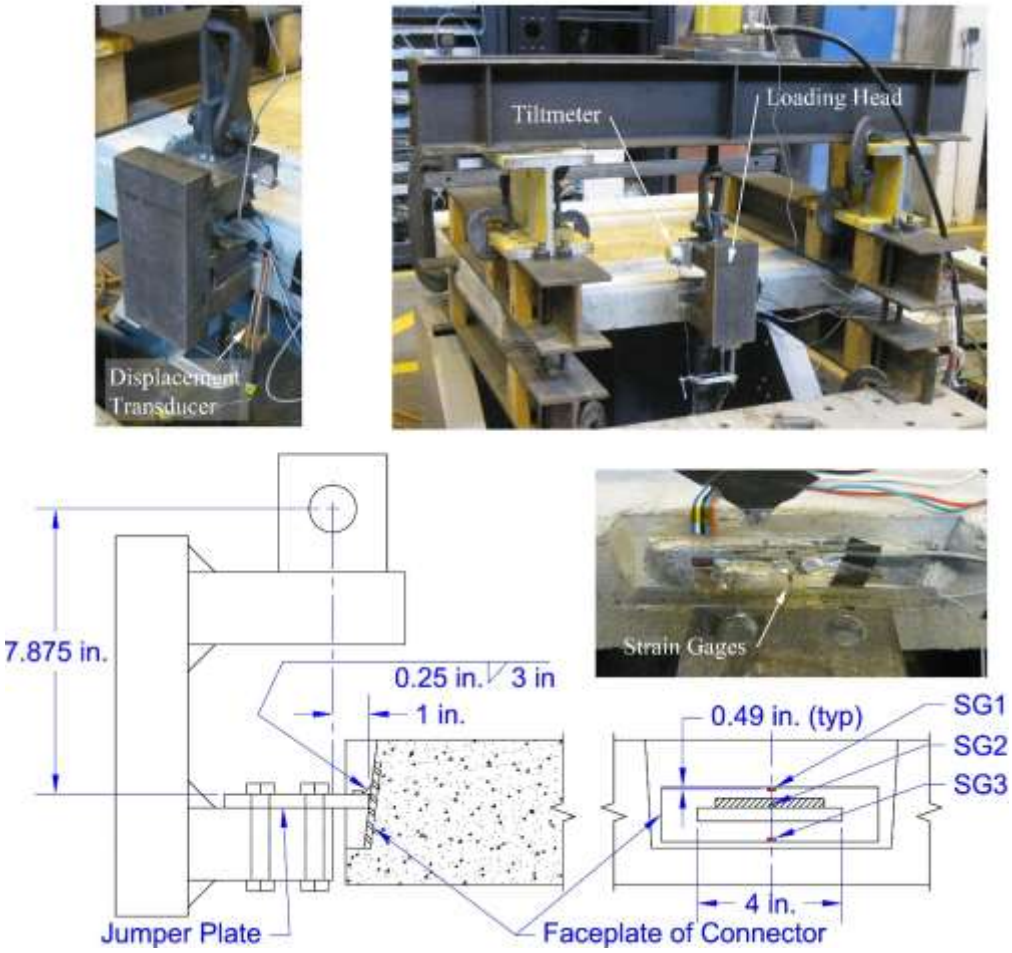

Figure 6: Overall single connector test setup details

The twelve tests were conducted on the three connector manufacturers identified as Manufacturer 1 (M1), Manufacturer 2 (M2) and Manufacturer 3 (M3) as illustrated in Figure 3. A carbon steel and stainless steel variation of each connector was evaluated. Each connector type was tested once in an upward direction (corresponding to tension at the root of the weld) and once in a downward direction (corresponding to closing of the gap between the slug and connector faceplate). These directions represent the general response that would occur on the left and right side of the jumper plate due to vertical loading (see Figure 4e). The test results are presented in Table 1. Concrete compression tests were

conducted prior to the start of the testing program and at the end of the testing program in accordance with ASTM C39[18]. The compressive strength ranged from 5700±380 psi to 6230±50 psi for the carbon steel connection tests and 5510±420 psi to 5980±520 psi for the stainless steel connection tests. The concrete compressive strength for each connector test was linearly interpolated based on the age of the panel relative to the cylinder test dates and is included in Table 1. The strength of the connector in each direction is noted along with the associated deformation. Due to a varying initial stiffness the applied load at a deformation of 0.010 in. is reported over that of an initial stiffness.

Table 1: Summary results

Connector	Direction	Estimated compressive strength [psi]	Applied Load at deformation of 0.010 in. [lbs]	Max Strength [lbs]	Deformation at Max Strength [in.]
M1 Carbon	Upward	5970	199	4418	0.119
	Downward	5980	398	7513	0.092
M2 Carbon	Upward	6550	1040	6270	1.225
	Downward	5900	195	6573	0.123
M3 Carbon	Upward	5900	294	7191	0.285
	Downward	5910	365	6828	0.118
M1 Stainless	Upward	5900	287	5084	0.121
	Downward	5940	143	6681	0.148
M2 Stainless	Upward	5800	259	8186	1.166
	Downward	5960	110	9174	0.564
M3 Stainless	Upward	5950	773	8241	0.274
	Downward	5950	597	7674	0.138

The vertical load - deformation of the connections in the upward and downward directions for the carbon and stainless steel connection are summarized in Figure 7. For clarity upward direction is shown as positive and downward direction as negative. A detailed summary of each test is provided in Naito and Hendricks[19].

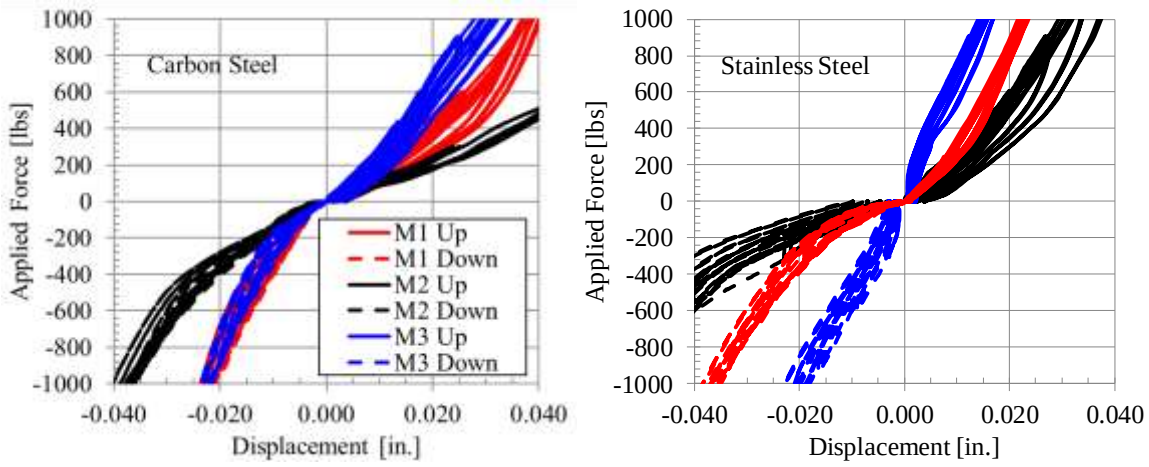

Figure 7: Vertical response of connectors – elastic range

3D Numerical Model Development

The connectors were tested individually as noted previously and are initially modeled as single sided to verify the accuracy of the FE model. Based on observations of the elastic performance in the experiments the concrete remains undamaged under the loads of interest. Two model types were created to compare to the test data. A complete detail incorporating concrete embedment and contact was used for manufacturer 1 (Figure 8a) and a simplified approach was used to represent the embedment for manufacturer 2 (Figure 8b). The simplified approach facilitates rapid assessment and requires less modeling time. The simple assembly consists of a 3D model of the connector (Figure 8b). Any locations where concrete embedment would be present are replaced with elastic supports. A rigid block is included to model the contact between the back of the connector face and the concrete. Nodal ties were used to join the weld to the connector face and to the jumper plate. “Hard” contact with no friction was used to model the contact between the connector and concrete and the slug and the connector face. In the second model, the 3D connector mesh is embedded in a 3D concrete mesh as shown in Figure 8a. The connectivity between

the concrete and steel elements was accomplished through nodal ties up to the point where the connector legs return to the face of the concrete. The contact between the slug and connector and connector faceplate and concrete was modeled using frictionless “hard” contact. All models were meshed with quadratic brick elements (C3D20) for the connector and slug geometry and quadratic tetrahedral elements (C3D10) for the concrete. All material properties used in the connector model were linear elastic with a modulus of elasticity of 29,000 ksi and Poisson’s ration of 0.3 used for the steel elements and an elastic modulus of 4,400 ksi and Poisson’s ratio of 0.15 used for the concrete elements.

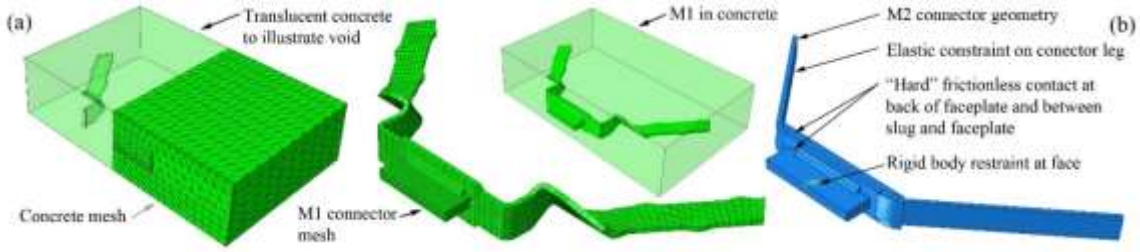

Figure 8: 3D FE model details (a) M1 connector, (b) M2 connector

3D Numerical Model Validation

The connection assemblies were modeled with load in upward and load in downward direction to match that of the experimental program. The measured vertical force versus measured vertical deflection are compared to the model results up to an applied vertical force of 525 lbs. The model shows good agreement for both Manufacturer 1 and 2 connectors as illustrated in Figure 9. The measured strains for strain gages SG1, SG2 and SG3 (see Figure 6) versus measured vertical deflection are compared to the modeled values for vertical deflections for the same range of load. The strain measurements are compared to the models for manufacturer 1 in Figure 10 and manufacturer 2 in Figure 11. In general, data from strain gages SG1, SG2, and SG3 compare well between the model and the test

data. The accuracy of the model in computing both the global behavior and local strains validates the accuracy of both the simplified and complex modeling approaches.

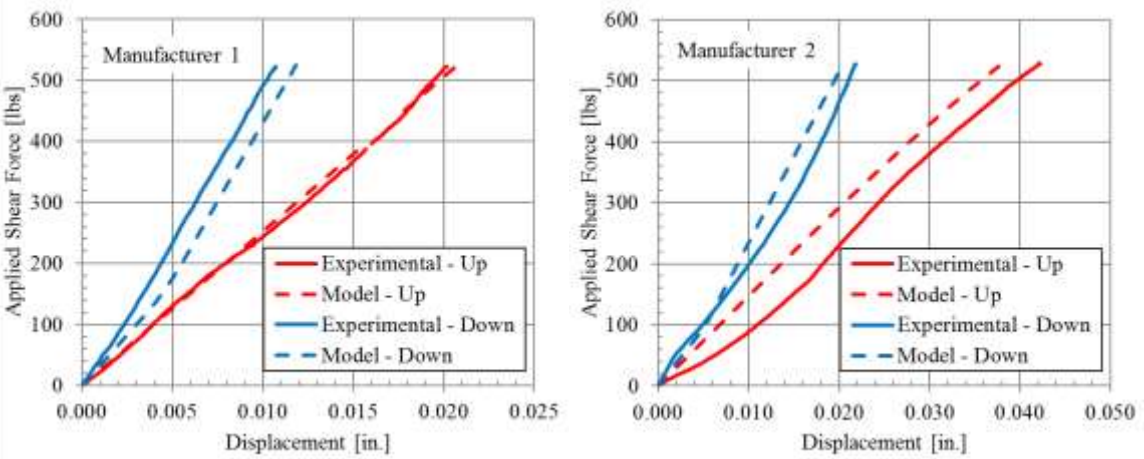

Figure 9: Comparison of numerical model with measured results for single sided loading

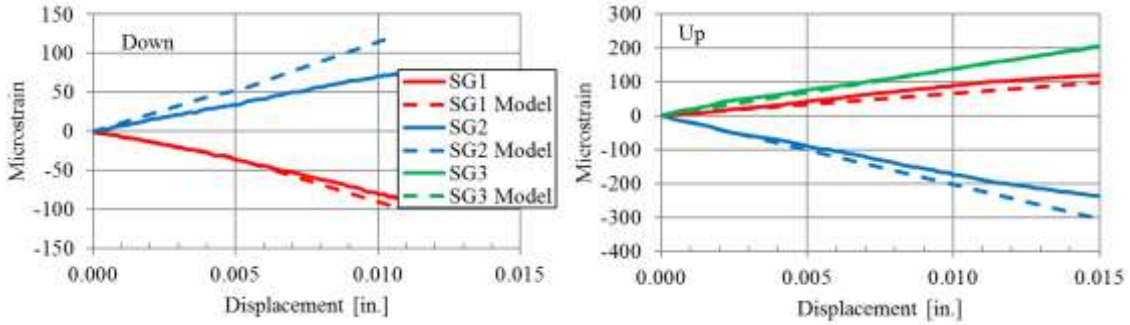

Figure 10: Comparison of numerical model with strain-displacement experimental results Manufacturer 1

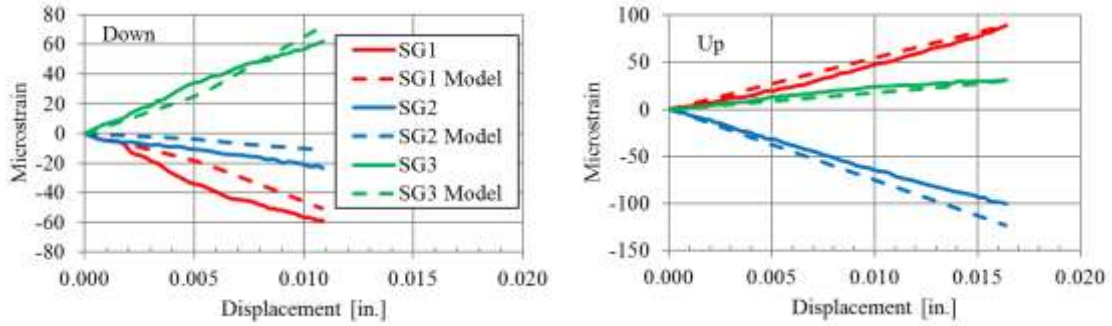

Figure 11: Comparison of numerical model with strain-displacement experimental results Manufacturer 2

DETERMINATION OF CONNECTION STIFFNESS

The FE models were extended from the single sided connection to the full flange to flange connection. The model was created by combining the upward and downward load models from Manufacturer 1 into a single assembly (Figure 12). The connector legs were embedded in a block with linear elastic concrete material properties. The connector was attached to the concrete by nodal ties along the embedded legs. Contact between the connector faceplate and concrete was modeled as “hard” frictionless contact. The element types used in the combined model were identical to those used in the M1 single sided model outlined above. To facilitate application of the nodal displacement and rotations obtained from the shell model of the diaphragm, the top and bottom surface nodes of the modeled concrete blocks were constrained to rigid body motion relative to a reference point at mid-height of the block immediately adjacent to the connector. The displacements and rotations used to determine the connector stiffness were applied directly to the concrete block reference point.

The stiffness components of the connector system were determined by subjecting the connector assemblies to the following load cases: Vertical shear deflection (K1), axial deflection (K2), and rotation about the weld longitudinal axis (K3). The physical interpretation of the stiffness components of the connector system is shown in Figure 13. The force or moment in the connection was plotted as a function of the deflection or rotation and were found to be linear for small deflections. The stiffness plots next to the corresponding deflected shape of the connector system are shown in Figure 14.

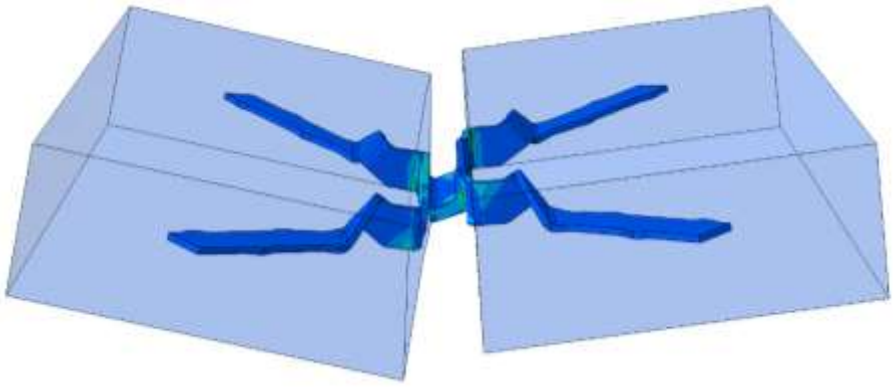

Figure 12: 3D FE model of connection in deformed position

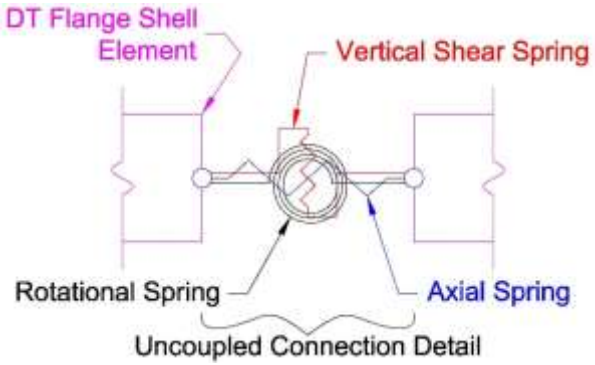

Figure 13: Uncoupled connection model

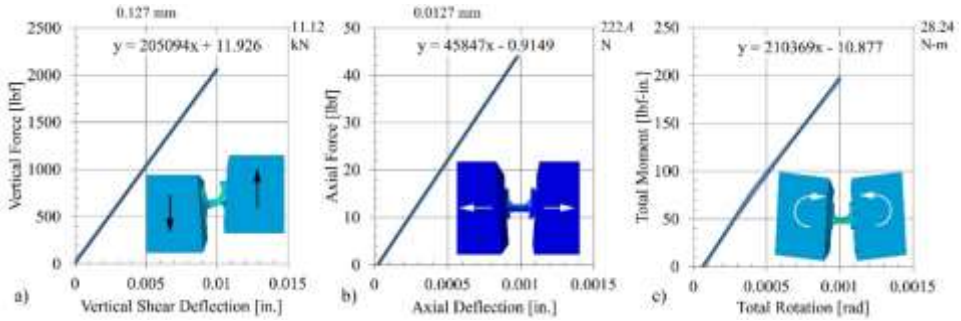

Figure 14: Component stiffness and deformed shapes of the M1 connector system, a) shear, b) tension, c) flexure

DEVELOPMENT AND VALIDATION OF 2D SHELL MODEL OF DIAPHRAGM

The stiffness for each connector type obtained from the 3D FE models was used to represent the behavior of the connections in a shell model of the floor diaphragm. The stiffness was input as a linear uncoupled link at the location of each connection. SAP2000[20] was used as the platform to create the shell model of the system. The model was created

using thin shell elements for both the double tee deck and legs. A 4 in. thick flange is used, typical of a pretopped double tee. The DT stem width was assumed as constant to simplify the model, with the width chosen to match the gross moment of inertia of the section. An illustration of the model of a three DT system using SAP2000 is illustrated in Figure 15.

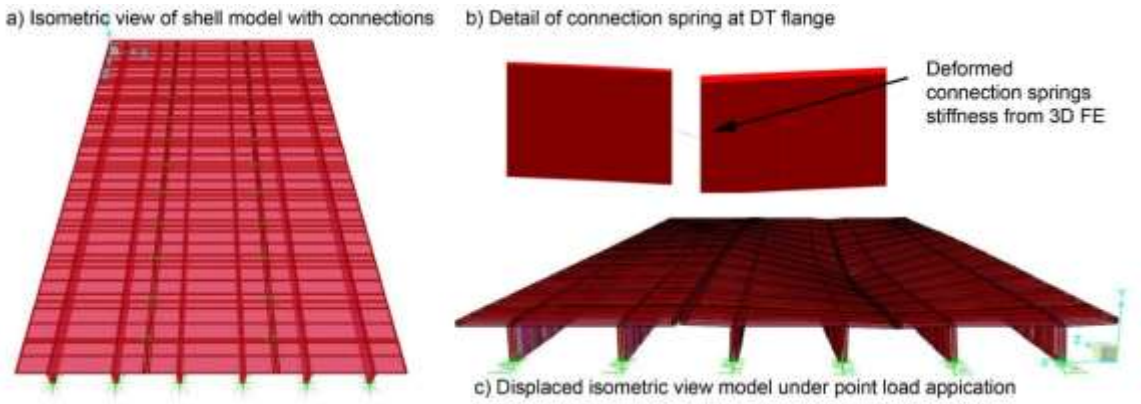

Figure 15: Overall View of SAP2000 shell/spring model

Coupled Shell Model 3D FE Model Validation

The final step of the proposed modeling approach imparts the vehicular loads to the shell model, measures the connector link deformations and applies these displacements to the 3D FE model of the connection. To verify the accuracy of this approach the model is compared to experimental test results conducted on full scale DTs by Lucier et al.[21]. The experiment consisted of point load application to three double tee beams positioned side by side. The connectors from Manufacturer 1 and Manufacturer 2 were used in the test setup. The test setup was comprised of three 60 ft 12DT30 double tees with the connectors along one joint from Manufacturer 1 and the connectors along the other joint from Manufacturer 2. The double tee system was subjected to point loads placed at different locations to determine the system response. During each load case, global deflections were monitored in nine locations and the strain response of five locations on several connectors

was measured. Point loads up to 3,000 lbs were applied to the double tees on each side of and directly adjacent to each connector. The connectors on each side of the middle double tee were designated B and C, with M1 connectors on line B and M2 connectors on line C. Load cases were designated Bi, Bo, Ci, and Co where Bi represents loading on the inside of connector line B and Bo represents loading on the outside of connector line B. Connectors were also labeled by their location along the length along the double tee in feet. As an example, load case Bo-27.5 indicates that the load was applied on the outside of connector joint B at the connector 27.5 feet from the end of the double tee. The double tee layout and loading locations examined in this paper are illustrated in Figure 16. A photograph of the test setup is shown in Figure 17. Details of the test setup and results are presented in detail in Lucier et al.[21] Data gleaned from the tests was used to develop and refine detailed finite element models and the iterative approach presented here.

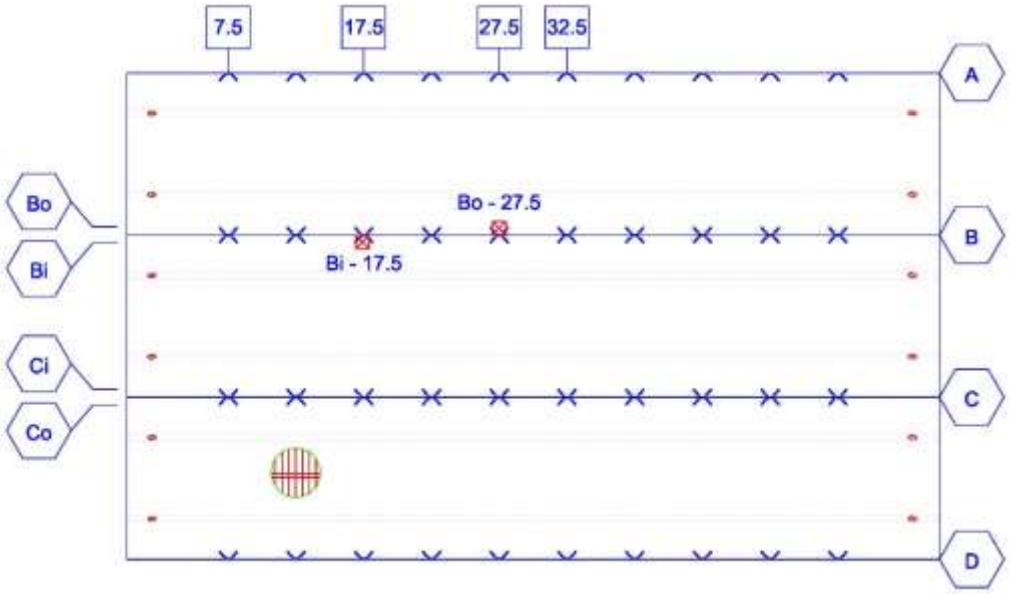

Figure 16: Full scale DT setup

Figure 17: Testing setup on full-scale DTs for load application Bi-7.5

A shell model of the full-scale test was developed as illustrated in Figure 15. An isometric view of the un-deformed (a) and deformed model (c – scale factor 500), and connection spring detail (b) is shown. A modulus of elasticity of 4,400 ksi and Poisson's ratio of 0.15 were used for the concrete. The boundary conditions of the diaphragm included a longitudinal spring at bearing support with an axial stiffness of 107 kip/in. to match the restraints observed in elastic tests of the double tee.

Determine Shear Force and Relative Deflections in Connections

The shell element model of the test setup is compared to measured deformations for six load cases. A 1.5 kip point load was applied at six load patches to determine the estimated deformation across the joint adjacent to the load. A comparison of the model and measured deformations are summarized in Table 2. As noted, three load cycles were applied to the DT panels. Significant variation was observed in the test between each load application, however the model provides a comparable estimate of deformation.

Table 2: Connector forces and differential deflections from SAP2000 model			
Load Case	Estimated connector force at load point [lbs.]	Estimated differential deflection [in.]	Measured differential deflection for three load cases and (average) [in.]
Bo-17.5	610	0.003	0.004, 0.0040, 0.004 (0.004)
Bi-17.5	590	0.004	0.006, 0.006, 0.007 (0.006)
Bo-27.5	510	0.003	0.001, 0.003, 0.002 (0.002)
Bi-27.5	520	0.004	0.006, 0.003, 0.005 (0.005)
Bo-30.0	NA	0.009	0.007, 0.008, 0.008 (0.008)
Bi-30.0	NA	0.010	0.014, 0.015, 0.015 (0.014)

To further validate the model, the relative deformations from the diaphragm model were applied to the detailed 3D FE model of the connector system. The measured and modeled strains were compared for the Bo-27.5 load case. Five strain gages (SG1-SG5) were installed at the connections as illustrated in Figure 18. The comparison was made by bounding the measured strains from gages SG2, SG4 and SG5 between the nodal strains from the analysis taken in the region where the strain gages were applied (see Figure 19). As illustrated in the FEA contours the strain varies significantly over the length of the strain gage in these regions. Consequently the range of FE values in the region are compared to the measured strain gage data. The measured strains were mostly bounded by the finite element model which indicates that the modeling approach is an adequate representation of the mechanics of the real system.

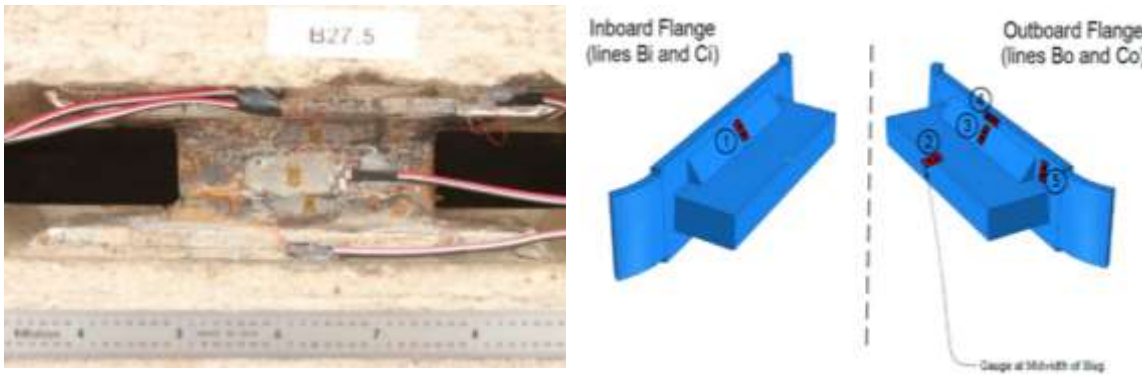

Figure 18: Photograph of connector B27.5 and schematic of strain gauge locations

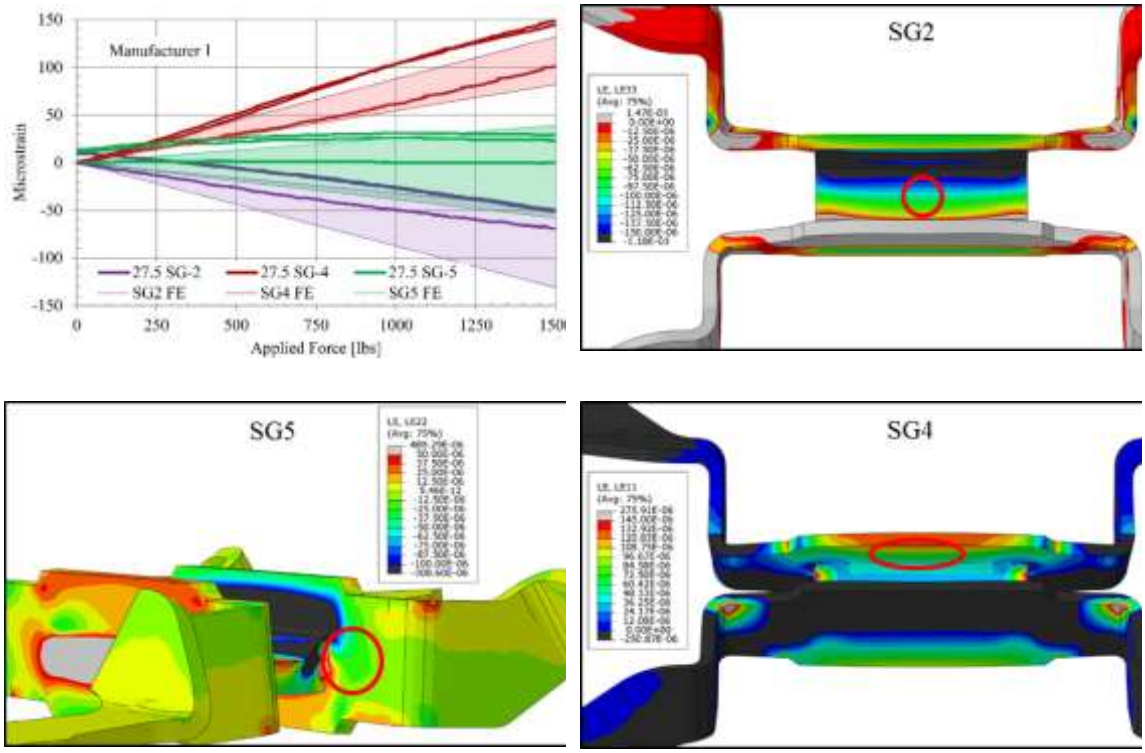

Figure 19: Comparison of Measured and Modeled Strains for Load Case T-Bo-27.5

DETERMINATION OF STRESS DISTRIBUTION IN CONNECTION

The connection deformations determined from the shell model can be applied to the 3D FE model to assess the state of stress in the weld as a result of the applied loading on the diaphragm. The Von Mises stress at various components of the connection are illustrated in Figure 20 .The results indicate that under a point load application to the floor, the stress

distribution in the connection varies considerably along the length of the weld and along the weld throat. Note the variation in Von Mises stress on the vertical face of the weld. The root of the weld on the downward deflected side (left) has a tensile stress, while the root of the weld on the side with the slug in contact with the connector is in compression. The approach used in this study facilitates evaluation of the peak stresses in the connection which can be used to assess fatigue life.

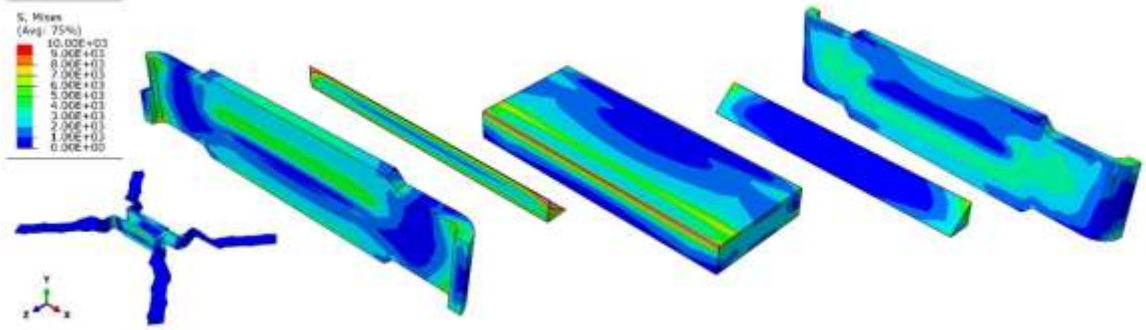

Figure 20: Von Mises stress distribution through connection

CASE STUDIES

To illustrate the application of the approach outlined in the paper two case studies are conducted. The first examines the effect of weld penetration on the stresses in the weld and the second examines the sensitivity of the connection to variations in double tee size.

Influence of Weld Penetration on Weld Stress

Proprietary connections are typically designed with a draft on the faceplate, with the top of the faceplate leaning back into the flange. This design detail creates a V-shape between adjacent connectors when the tees are installed. The shape facilitates placement of jumper plates by minimizing the likelihood for the slug to drop-through to the floor below when installed for welding. The draft of the faceplate creates a gap between the top of the jumper

plate and the faceplate. During welding this gap may or may not be filled with molten weld material. Two sections removed from the full scale tests indicates that weld penetration is likely (see Figure 21).

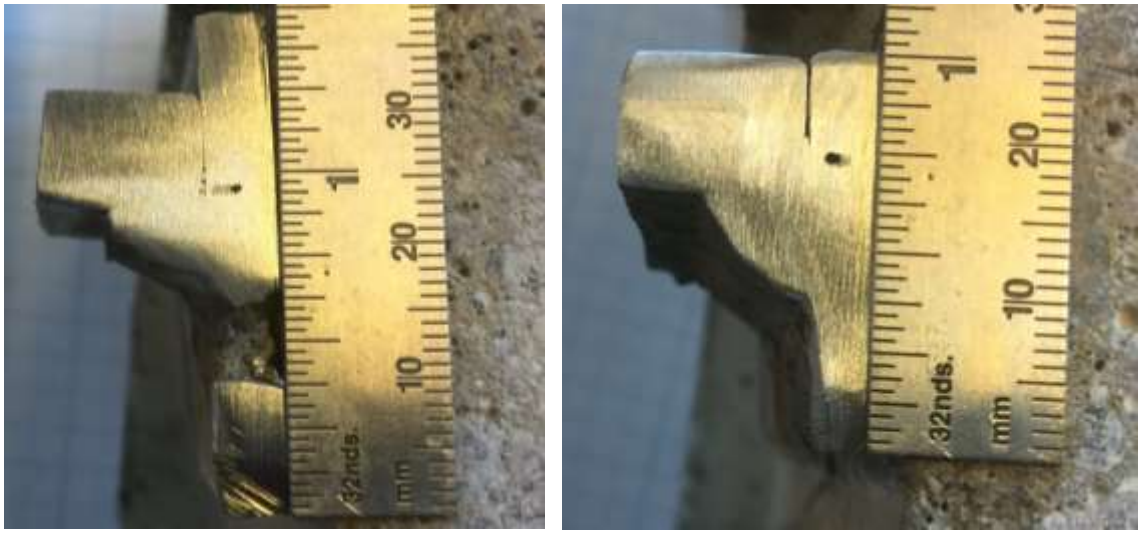

Figure 21: Weld penetration between jumper plate and faceplate on M1 connector (left) and M2 connector (right)

To examine the sensitivity to weld penetration three 3D FE models are evaluated. The applied displacements and rotations were identical for all models, and the effects of weld penetration on the stiffness components of the connector were not examined. The welds in the previously modeled connections have been idealized as a triangular cross section. Actual field welding on connectors could be expected to have some penetration of weld metal into the gap between the jumper plate and connector face due to the draft of the connector faceplate. The effects of weld penetration would be expected to decrease the stresses at the root of the weld for the same applied load. To illustrate this effect the connection is modeled with three levels of penetration: No weld penetration (idealized triangular weld cross section), 0.0783 in. of penetration, and 0.1568 in. of penetration as

illustrated in Figure 22.

Penetration of weld metal into the slug/faceplate gap increases the effective throat of the fillet weld and consequently reduces the stress levels in the weld. The maximum principal stress distribution along the weld at the centerline of the weld face are shown in Figure 23a. The analysis indicates that the principal stress level at the mid-surface of the weld varies linearly as a function of the inverse of the effective throat length squared. Where the effective throat is measured as the distance from the bottom of the weld to the centerline of the face of the weld as shown in Figure 23b. A comparison of the strains recorded for SG3 (Figure 18) for load case Bo-27.5 show that increasing the level of weld penetration causes the modeled strain to more closely match that measured during the test (See Figure 24) . For load case Bo-27.5, SG3 is on the side of the connection where the weld root is in tension (the gap between the connector face and slug is opening). SG1 is on the closing side of the connection and measured essentially no strain. This also correlates well with the model, which predicts less than 5 microstrain at the weld face regardless of the level of weld penetration. The correlation between lower weld stress levels and weld penetration is an important aspect in assessing the fatigue life of connections.

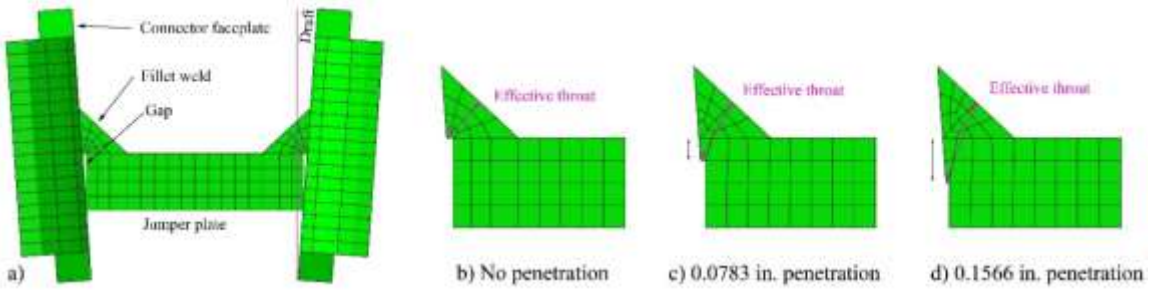

Figure 22: Weld profiles with mesh with varying levels of weld penetration. The effective throat length is shown in red.

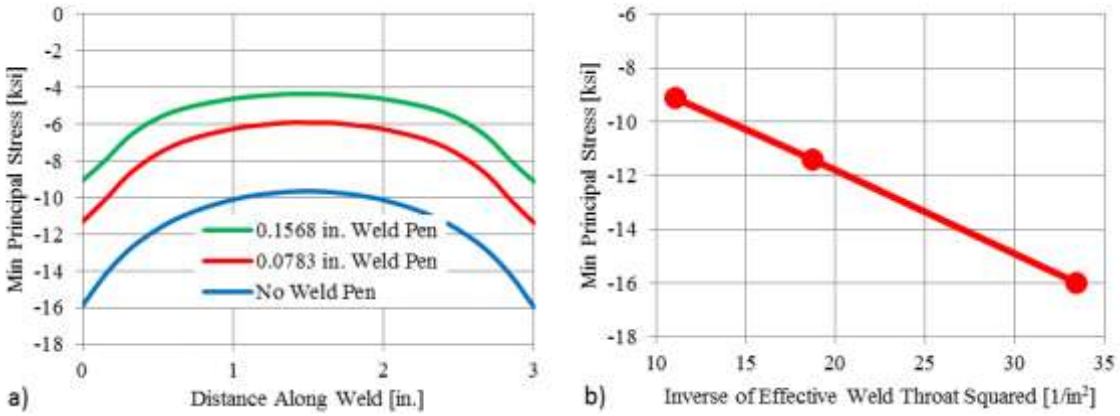

Figure 23: Variation of maximum principal stress at mid-face of weld with varying levels of weld penetration

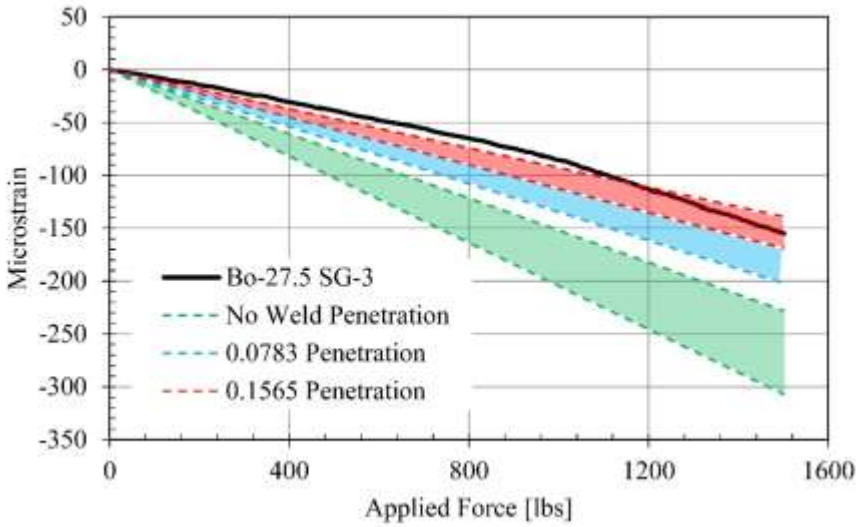

Figure 24: SG3 with comparison of modeled strains for varying levels of weld penetration

Influence of Double Tee Size on Connections

A case study was conducted to examine the effect of DT size on the relative connection forces and stresses. Three double tees were examined: 10DT34, 12DT30, and 15DT30. The connection spacing for each double tee matched that of the full scale tests (Lucier et al.[21]). The relative DT sizes are shown in Figure 25 (left). The model consisted of three side by side double tees with M1 connectors. The slug size was 3 in. x 1 in. x 3/8 in. and the mid-

height of the slug was at the mid-height of the flange. The fillet weld size on both sides of the connection was ¼ in. and was 2.5 in. long as recommended by the connector manufacturer. This connector configurations corresponds to the connector component stiffness analysis shown in Figure 14.

The applied load was developed from an EPA study on vehicle trends[22]. The average 2015 production vehicle (average of all trucks and cars) was chosen. The average weight of the vehicle is 4035 lbs including a 300 lbs occupant load. The average footprint (wheel base by track width) was 49.4 ft^2. Assuming a wheel base to track width ratio of approximately 1.6 and averaging to the nearest inch resulted in four point loads placed at a track width of 66 in. and wheel base of 105 in. Assuming an equal 50/50 ratio of wheel loads to the front and rear axle results in a 1009 lbs point load at each location. The vehicle was placed with the centerline of the wheels 3.0 in. from the joint with the vehicle straddling midspan of the double tee. This loading configuration puts the front wheels just outside the two connectors closest to the double tee mid-span and represents a near worst case loading scenario. As illustrated the connection force magnitude is most sensitive to local bending of the free edge of the flange and varies as a function of the inverse cube of the free flange length (the distance between the double tee stem and the free edge of the flange, see Figure 25 (right) and Figure 26. This conclusion is supported by the observation that as the moment of inertia increases from the 12DT30 to the 15DT30 the connection forces also increase. Furthermore, as the distance from the stem to the edge of the tee decreases from the 15DT30 to the 12DT30 and 10DT34 the local flange stiffness increases as demonstrated by the increase in both principal stress and connection force (see Figure 27 and Table 3).

This increase in local flange stiffness results in increased load being carried by global flexure of the loaded span with less force being transferred across all connections. Further parametric studies can be readily conducted with this method.

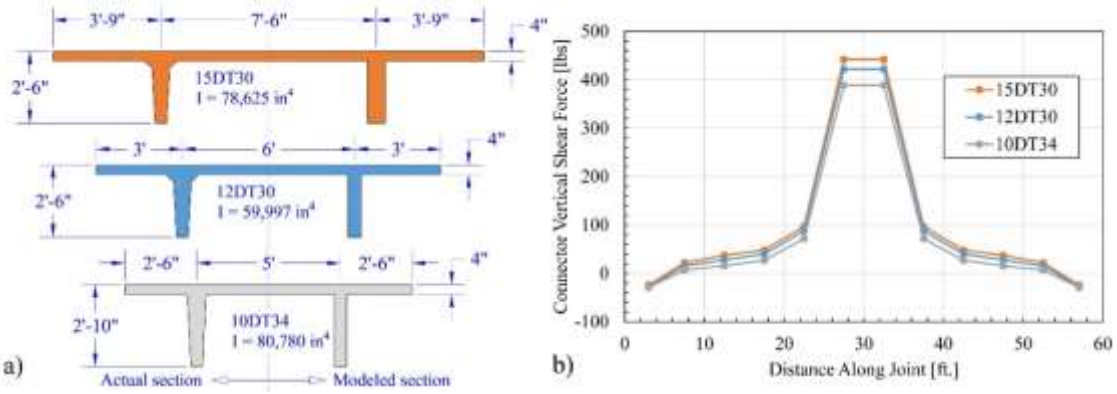

Figure 25: Connection force distribution in shell model for different DT sizes

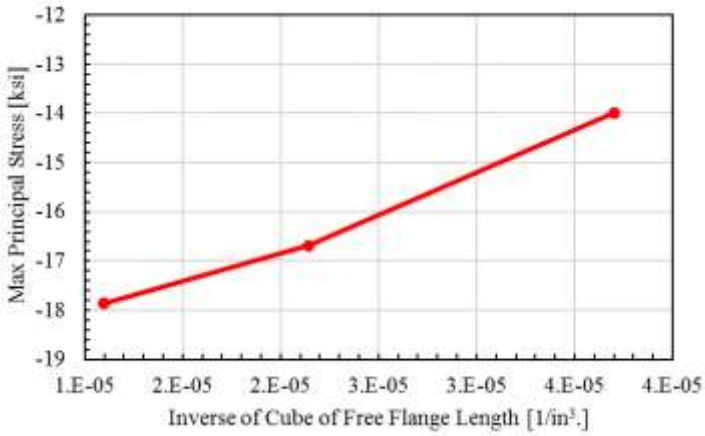

Figure 26: Effect of free flange length on connection stress

Table 3: Estimated response for case study

DT Size	Axial Deformation	Shear Deformation	Rotation on Load Side	Rotation on Other Side	Shear Force in Connection	Min Principal Stress
	[in]	[in]	[rad]	[rad]	[lbf]	[ksi]
10DT34	0.00061	0.00260	0.00028	-0.00065	389	-13.9834
12DT30	0.00040	0.00280	0.00040	-0.00085	422	-16.6855
15DT30	0.00004	0.00300	0.00420	-0.00810	442	-17.8617

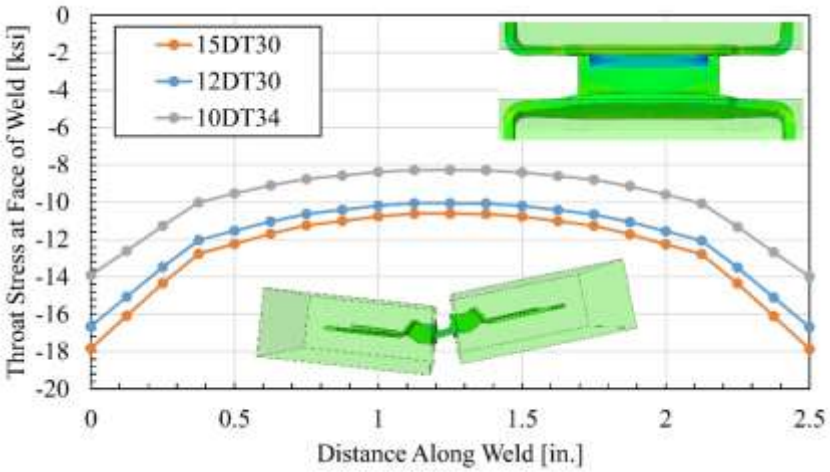

Figure 27: Midspan connection minimum principal stress variation along face of weld for different DT sizes

CONCLUSIONS

To properly assess the fatigue resistance of the connection requires a knowledge of: (1) the relationship between the applied vehicle load and the resulting stresses in the connection welds, (2) the expected vehicle demands and distributions in the structure over the expected service life, and (3) an S-N curve that is applicable for the weld being considered. A numerical and experimental study was conducted to examine part (1). An iterative numerical method is proposed that consists of detailed 3D FEA of the connection and surrounding embedment with a parallel shell element model of the diaphragm. Based on the work the following conclusions can be made:

- The stress in the weld cannot be determined by simplified engineering assumptions and requires finite element analysis methods to accurately determine the magnitude and distribution.
- The modeling methods are shown to accurately capture the complex mechanics of the connector system by comparison to test data.
- The connector stresses are dependent on the specific connector configuration, including the connector type and slug and weld dimensions.

- The force level and corresponding stresses in connections are influenced by local bending of the double tee flange and varies as a function of the inverse cube of the free flange length and so modeling must account for the diaphragm system double tee properties, especially the free flange length.
- The stresses in welds can vary significantly depending on the amount of weld metal penetration into the gap between the slug and connector. Weld penetration increases the effective throat length of the weld and the stress level varies with the square of the effective throat length. Failure to account for weld penetration will result in a significant over estimation of weld stresses.
- The methods outlined here, when combined with an accurate vehicular loading spectrum and appropriate fatigue life curve for fillet welds subject to tension at the root, will allow for accurate fatigue life analysis of precast double tee systems.

REFERENCES

1. Naito, C., Osborn, A., Rahmani, E. & Hendricks, R. Double Tee Flange Connections – Analytical Evaluation. *2017 PCI Conv. Natl. Bridg. Conf.* Paper 99 (2017).
2. Venuti, W. J. Diaphragm Shear Connectors Between Flanges of Prestressed Concrete T-Beams. *PCI J.* 67–78 (1970).
3. Spencer, R. A. & Neille, D. S. Cyclic Tests of Welded Headed Stud Connections. *PCI J.* **21,** 70–83 (1976).
4. Aswad, A. *Comprehensive Report on Precast and Prestressed Connectors Testing Program*. *Stanley Structures Report* (1977).
5. Pincheira, J. A., Oliva, M. G. & Kusumo-Rahardjo, F. I. Tests on double tee flange connectors subjected to monotonic and cyclic loading. *PCI J.* **43,** 82–96 (1998).
6. Oliva, M. G. *Testing of the JVI Flange Connector for Precast Concrete Double-Tee Systems*. *University of Wisconsin Structural Materials and Testing Lab Report* (2000).
7. Wiss Janey Elstner and Associates, I. *Dayton/Richmond Flange-to-Flange Connector Tests*. (2002).
8. Shaikh, F. A. & Feile, E. P. Load Testing of a Precast Concrete Double-Tee Flange Connector. *PCI J.* **49,** 84–95 (2004).
9. Naito, C. *Erector Connector Meadow Burke Company In-Plane Performance*. *ATLSS Report No.06-22* (2007).
10. Naito, C. J. & Hendricks, R. *In-Plane and Out-of-Plane Performance of the MC Flange Connector*. *ATLSS Report No.08-08* (2008).
11. Ren, R. & Naito, C. Precast Concrete Diaphragm Connector Performance Database. *J. Struct. Eng.* **139,** 15–27 (2013).
12. Naito, C., Cao, L. & Peter, W. Precast concrete double-tee connections, part 1 : Tension behavior. 49–66 (2009).
13. Cao, L. & Naito, C. Precast concrete double-tee connections, part 2 : Shear behavior. *PCI J.* 97–115 (2009).
14. Naito, C. & Ren, R. An evaluation method for precast concrete diaphragm connectors based on structural testing. *PCI J.* 106–118 (2013).
15. Klein, G. & Lindenberg, R. *Volume Change Movement and Forces in Precast Concrete Buildings*. *WJE No.2002.1117* (2009).
16. PCI Connections Details Committee. *PCI Connections Manual*. *MNL 138-08* (2008).
17. Dassult Systems. ABAQUS Finite Element Software, Ver. 6.13. (2016).
18. ASTM C39. Standard Test Method for Compressive Strength of Cylindrical Concrete Specimens. *Am. Soc. Test. Mater.* **C,** 1–7 (2014).
19. Naito, C. J. & Hendricks, R. *PCI Fatigue Study: Experimental Evaluation of Double Tee Flange Connectors Subject to Out-of-Plane Loading*. *ATLSS Report No.16-07* (2016).
20. Wilson, E. L. & Habibullah, A. SAP2000 integrated finite element analysis and design of structures. *Computers and Structures* (1997).

21. Lucier, G., Naito, C., Osborn, A., Nafadi, M. & Rizkalla, S. Double Tee Flange Connections – Experimental Evaluation. in *2017 PCI Convention and National Bridge Conference* Paper 98 (2017).
22. Technology, L. A. & Emissions, C. D. Light-Duty Automotive Technology, Carbon Dioxide Emissions, and Fuel Economy Trends: 1975 Through 2016. (2016). doi:10.1002/yd.282

VITA

Robin Hendricks was born in Kempton, Pennsylvania on December 30, 1984 to Steven and Denise Hendricks. He graduated from Kutztown University in Kutztown, Pennsylvania in May, 2008 with a Bachelor of Science in Physics. He has worked as a Research Scientist in the ATLSS Engineering Research Center since May, 2008.